

Gas-phase energetics of organic free radicals using time-resolved photoacoustic calorimetry

Catarina F. Correia^a, Paulo M. Nunes^a, Rui M. Borges dos Santos^{b,1},
José A. Martinho Simões^{a,*}

^a Departamento de Química e Bioquímica, Faculdade de Ciências, Universidade de Lisboa,
1749-016 Lisbon, Portugal

^b Faculdade de Engenharia de Recursos Naturais, Universidade do Algarve, Campus de Gambelas,
8005-139 Faro, Portugal

Received 30 August 2003; accepted 20 October 2003
Available online 4 August 2004

Abstract

A generalized method for the determination of thermochemical data of transient species, using time-resolved photoacoustic calorimetry (TR-PAC), is described in detail. Taking phenol as an example, the procedure for the determination of the PhO–H bond dissociation enthalpy from photoacoustic experiments, in various solvents, is presented, and its assumptions discussed. To derive gas-phase bond dissociation enthalpies from the solution values, a widely used procedure is compared with a computational chemistry (CC) microsolvation method. Results from the combined TR-PAC/CC approach show that the established “hydrogen bond only” model (to describe the difference between the solvation enthalpies of phenol and phenoxy radical) leads to an underestimation of the derived gas-phase bond dissociation enthalpy. When that differential solvation is properly accounted for, the agreement between our results and a recommended gas-phase value improves, indicating that the combined TR-PAC/CC approach is a valid tool for the study of organic free radical energetics.

© 2004 Elsevier B.V. All rights reserved.

Keywords: Thermochemistry; Time-resolved photoacoustic calorimetry; Solvation; Phenol; Bond dissociation enthalpy

1. Introduction

Time-resolved photoacoustic calorimetry (TR-PAC) is a recent technique that is being established as a tool for the determination of bond dissociation enthalpies in solution [1,2]. It represents a development of the classical (non-time-resolved or static) PAC, already a well-known technique in the same area [3], but which does have some limitations. In both cases the experimental strategy usually involves the cleavage of the bond of interest through a suitable reaction which, in the case of classical PAC, has to be very fast (typically with an overall duration in the nanosecond time scale). TR-PAC not only eliminates this requirement, but it also provides kinetic information in addition to the enthalpic data. In this work we used time-resolved

photoacoustic calorimetry to determine the O–H bond dissociation enthalpy of phenol in several solvents, as a general example of the procedure, and to illustrate the advantages of the time-resolved vs. the classical version of the technique. A crucial part of the study of bond dissociation enthalpies is the relation of the experimentally determined solution results with gas-phase values. Its importance for hydrogen-bonding molecules, and for phenol in particular, has been pointed out, and several related methods to deal with this issue have been presented [4,5]. However, we recently found that the validity of those methods is not general, and that more sophisticated models, making use of computational chemistry calculations (CC), are needed to afford accurate results [6,7]. In the following sections we will analyze the combined TR-PAC/CC approach in this context. The experimental setup and general procedure will be presented, and the algorithms used to yield thermodynamic data will be described in some detail, so as to discuss the main assumptions and approximations of the method.

* Corresponding author. Tel.: +351 217500005; fax: +351 217500088.
E-mail address: jams@fc.ul.pt (J.A. Martinho Simões).

¹ Co-corresponding author.

2. Experimental

2.1. Materials

Benzene (Aldrich), acetonitrile (Aldrich) and carbon tetrachloride (Aldrich) were of HPLC grade and used as received. Di-*tert*-butylperoxide (Aldrich) was purified according to a literature procedure [8]. *tert*-Butanol (Merck) was dried over calcium hydride, fractionally distilled, and kept in a glove box over calcium. Phenol (Aldrich, +99%) was sublimed in vacuum and kept under nitrogen prior to use. *ortho*-Hydroxybenzophenone (Aldrich) was recrystallized twice from an ethanol-water mixture. Ferrocene was prepared according to the literature [9] and purified by double sublimation in vacuum.

2.2. Photoacoustic calorimetry

2.2.1. Theory of photoacoustic calorimetry

The theoretical basis of photoacoustic calorimetry has been widely discussed before [10,11], but an outline is provided here. The PAC technique involves the measurement of a volume change that occurs when a laser pulse strikes a solution containing the reactants and initiates a chemical reaction. This sudden volume change generates an acoustic wave, which can be recorded by a sensitive microphone such as an ultrasonic transducer. The resulting photoacoustic signal, S , is defined by Eq. (1), where T is the solution transmittance, E the incident laser energy, and K the calibration constant, dependent on the instrumental specifications and geometry, and on the thermoelastic properties of the solution.

$$S = K\phi_{\text{obs}}(1 - T)E \quad (1)$$

The parameter ϕ_{obs} is the apparent fraction of photon energy released as heat, which, when multiplied by the molar photon energy ($E_{\text{m}} = N_{\text{A}}h\nu$), corresponds to the measured apparent enthalpic change, $\Delta_{\text{obs}}H = \phi_{\text{obs}}E_{\text{m}}$. The use of the word “apparent” is justified as follows: it has been shown that ϕ_{obs} consists of a thermal contribution, due to the enthalpy of the reaction, and a reaction volume contribution, due to the differences between the partial molar volumes of the reactants and products [12]. The latter leads to the introduction of a correction factor when calculating the reaction enthalpy through an energy balance [11,13], Eq. (2).

$$\Delta_{\text{r}}H = \frac{E_{\text{m}} - \Delta_{\text{obs}}H}{\Phi_{\text{r}}} + \frac{\Delta_{\text{r}}V}{\chi} \quad (2)$$

In this equation, Φ_{r} represents the reaction quantum yield. The correction term includes the reaction volume change, $\Delta_{\text{r}}V$, and the adiabatic expansion coefficient of the solution, χ . Since the solutions used are usually very diluted, this parameter depends on the thermoelastic properties of the solvent (however, see Section 2.2.2), namely the isobaric expansion coefficient, α_{p} , the heat capacity, C_{p} , and the density, ρ , Eq. (3).

$$\chi = \frac{\alpha_{\text{p}}}{\rho C_{\text{p}}} \quad (3)$$

Eq. (1) is the basis of classical photoacoustic calorimetry. As stated in the Introduction it is usually called non-time-resolved PAC, in the sense that the time dependence of the signal S is not analyzed (see below). Its application is valid only when the process generating the photoacoustic signal is much faster than the transducer response [14]. This is the time constraint of classical PAC, and can be written as $\tau \ll 1/\nu$, where τ represents the lifetime of the process and ν is the characteristic frequency of the microphone. Only in this case will the time-profile of the photoacoustic wave depend exclusively on the instrumental response, and not on the rate of the process, allowing the direct correspondence between its amplitude S and the apparent heat fraction ϕ_{obs} . On the other hand, processes that are much slower than the transducer response ($\tau \gg 1/\nu$) will give rise to virtually no signal. In the intermediate regime ($\tau \approx 1/\nu$), each process with a different rate will originate a unique waveform. For instance, in a system where one or more of such processes occur, the signal obtained will be a convoluted waveform that will appear phase-shifted and reduced in amplitude due to the presence of components corresponding to slower reactions. A deconvolution analysis of such data yields the magnitude of each of the signal-inducing events (as well as information on their rates) [15]. This is the basis of time-resolved photoacoustic calorimetry (TR-PAC). The analysis involves the normalization of the photoacoustic waveform for its respective absorbance ($1 - T$) and incident laser energy E , as indicated in Eq. (1). Extraction of ϕ_{obs} for the process(es) is then accomplished by the deconvolution of the waveform, facilitated by the use of commercially available software [16]. Reaction enthalpies for each process are then calculated as before [10c]. For instance, considering a two step sequential reaction, the enthalpy of the first step (photochemical) is given by Eq. (2) (with $\Delta_{\text{obs}}H = \Delta_{\text{obs}}H_1$, calculated from the amplitude $\phi_{\text{obs},1}$ obtained from the deconvolution, and $\Delta_{\text{r}}V = \Delta_{\text{r}}V_1$). The enthalpy of the second step (thermal) is calculated with Eq. (4) (note that only the first step is light-initiated but the yield of the sequential step is dependent on the quantum yield for the first one).

$$\Delta_{\text{r}}H_2 = \frac{-\Delta_{\text{obs}}H_2}{\Phi_{\text{r}}} + \frac{\Delta_{\text{r}}V_2}{\chi} \quad (4)$$

2.2.2. Instrumental setup and experimental procedure

Our photoacoustic calorimeter setup and experimental procedure have been described in detail elsewhere [1,11]. Briefly, argon-purged solutions of ca. 0.4 M of di-*tert*-butylperoxide and the substrate (phenol) in the adequate concentration (see Table 4) were flowed through a quartz flow cell (Hellma 174-QS). The solutions were photolysed with pulses from a nitrogen laser (PTI PL 2300, 337.1 nm, pulse width 800 ps). The incident laser energy was varied by using neutral density filters (ca. 5–30 $\mu\text{J}/\text{pulse}$).

at the cell, flux $<40 \text{ J m}^{-2}$). Each pulse induced a volume change in solution, producing an acoustic wave that was detected by a piezoelectric transducer (Panametrics V101, 0.5 MHz) in contact with the bottom of the cell. The signals were amplified (Panametrics 5662) and measured by a digital oscilloscope (Tektronix 2430A). The signal-to-noise ratio was improved by averaging 32 acquisitions. Each data point, at each of four different incident laser energies used, was determined five times. To check for multiphoton effects, the average signal was plotted against the laser energy (linear correlations with zero intercept have always been observed). The apparatus was calibrated by carrying out a photoacoustic run using an optically matched (within typically 6% absorbance units at 337.1 nm) solution of *ortho*-hydroxybenzophenone or ferrocene (photoacoustic calibrants) in the same solvent used in the experiment (this solution does not include the peroxide but contains also phenol, with the same concentration as in the experiment; see below). The above photoacoustic calibrants dissipate all of the absorbed energy as heat ($\phi_{\text{obs}} = 1$) [10b]. For each run (experiment or calibration), four data points were collected, corresponding to the four different laser intensities obtained using the neutral density filters. The resulting waveforms from each data point were recorded for subsequent mathematical analysis, affording three waveforms for each point: sample, calibration, and solvent (again containing the phenol in the same concentration as in the other two). After the normalization of the waveforms explained in Section 2.2.1, the analysis for each point involved the subtraction of the solvent signal from both the sample and calibration waveforms, and then their deconvolution using the software Sound Analysis by Quantum Northwest [16].

Subtraction of the solvent signal can be important because a significant background signal (from the solvent and/or substrate) may affect the deconvolution of the waveforms, which in essence depends on a fitting procedure (in extreme cases, it can even render the fitting impossible). Subtraction of the solvent waveform usually increases the accuracy of the deconvolution process (verified by an improvement of the “goodness of fit” through residuals and autocorrelation analysis). However, in the solutions used in the present work, the background signal was negligible, so this step was not necessary (as verified by the agreement between the results obtained before and after the subtraction of the solvent signal).

Another important issue regards the need to use substrate (phenol, in this case) in the calibration solution. An essential requirement of the PAC technique is that the thermoelastic properties of the calibration solution and the sample solution, namely their adiabatic expansion coefficients χ (Eq. (3)), should be identical. Since the solutions used are normally very diluted, it is generally assumed that both will have χ equal to that of the pure solvent. There has been a doubt as to whether this assumption is valid, due to the fact that the sample solution contains ca. 6% (v/v) of di-*tert*-butylperoxide, whereas the calibration so-

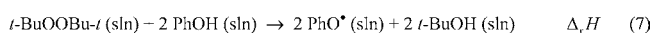
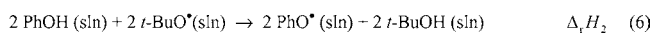
lution contains none. In fact, it has been shown that using methanol as the solvent, both the amplitude and arrival time of the acoustic wave vary between the reference and the sample containing 15% peroxide, demonstrating a change in the thermoelastic properties [17]. However, using benzene, isooctane, carbon tetrachloride, and acetonitrile as solvents, all the available evidence seems to corroborate the assumption above: the shape and time of arrival of the photoacoustic waveform is the same for calibration and experiment, and increasing the amount of peroxide in the sample solution does not noticeably affect the time of arrival of the photoacoustic waveform. Moreover, and which is a more rigorous test, a plot of the photoacoustic signal versus the amount of peroxide added during the experiment remains linear even beyond 12% (v/v) of peroxide in solution [18].

2.3. Reaction–solution calorimetry

The enthalpies of solution of *tert*-butanol and di-*tert*-butylperoxide in benzene, carbon tetrachloride, and acetonitrile containing 4–7% (v/v) of di-*tert*-butylperoxide and different concentrations of phenol (see Table 3) were determined with an isoperibol reaction–solution calorimeter [19]. The results refer also to 298.15 K.

3. Results and discussion

The general strategy for determining the R–H bond dissociation enthalpy in an organic molecule using photoacoustic calorimetry, is illustrated in Scheme 1. A *tert*-butoxy radical generated from the photolysis of di-*tert*-butylperoxide (reaction 5) abstracts a hydrogen atom from the substrate (phenol in this example), yielding the corresponding radical (phenoxy in reaction 6). Reaction 7 represents the net process.



Scheme 1.

The slower process in Scheme 1 is the hydrogen abstraction with the *tert*-butoxy radical (since reaction 5 is, in practical terms, instantaneous). The lifetime τ of this reaction is related to its pseudo first-order rate constant $k[\text{PhOH}]$, and can be set by choosing the adequate concentration of phenol, Eq. (8).

$$\tau = \frac{1}{k[\text{PhOH}]} \quad (8)$$

Eq. (8) shows that it might be possible to meet the time-constraint of classical PAC (see Section 2.2.1) by using a high enough concentration of substrate. For our

0.5 MHz transducer, and in the case of phenol in benzene, the condition is satisfied by using a concentration greater than 0.06 M^2 [11]. However, due to the kinetic solvent effect [20], when acetonitrile is used instead of benzene the rate constant of reaction 6 is at least ca. 30 times slower,³ placing the experiment on the edge of applicability of the non resolved technique.⁴ If the objective were to cleave the benzylic C–H bond in toluene, even with neat toluene this process would fall in the intermediate regime [2], and classical PAC could no longer be used in the form described above. There is a more elaborate procedure, which, by using competing reactions, enables the use of classical PAC even in this case. However, it requires prior information for the system under study (either the rate constants or the enthalpies of the reactions involved) [3]. In our view, TR-PAC represents a simpler, more direct approach. It is also more versatile: it does *not* require the previous knowledge of the rate constant of reaction 6 for obtaining the enthalpy of the process, and it even allows the simultaneous determination of its lifetime τ . While that is not our goal, one could use TR-PAC for the kinetic study of reaction 6 with different substrates (using the same experimental setup but a somewhat different procedure) [21].

Summing up, using TR-PAC, the deconvolution of the photoacoustic waveforms obtained from the study of Scheme 1 affords the amplitudes (ϕ_{obs}) of the two elementary steps and the lifetime (τ) of the second [10c]. Only reaction 6 is of concern to us here. Its enthalpy ($\Delta_{\text{r}}H_2$) can be calculated from Eq. (9), derived from Eq. (4) by assuming that the volume change ($\Delta_{\text{r}}V_2$) is negligible, which is sensible because the hydrogen abstraction is a metathesis reaction [4]. It should be pointed out that this represents a further advantage of TR-PAC over classical PAC, since it allows to avoid the volume correction presented in Eq. (2) (see, however, below).

$$\Delta_{\text{r}}H_2 = -\frac{\Delta_{\text{obs}}H_2}{\Phi_{\text{r}}} \quad (9)$$

In Eq. (9) Φ_{r} is the *t*-BuO–O \cdot –*t*-BuO \cdot homolysis quantum yield, which was experimentally determined in a number of sol-

vents [4], and found to correlate with their viscosities. This correlation reflects the fact that in more viscous media there is an increase in the number of molecules that cannot escape the “solvent cage” and therefore recombine, leading to a decrease in the quantum yield (the quantum yield in the gas-phase is unity). The correlation is very useful because it allows to predict Φ_{r} values in any solvent or mixture [2].

As the enthalpy of reaction 6 is simply twice the difference between the solution-phase O–H bond dissociation enthalpies of phenol and *tert*-butanol, $DH_{\text{sln}}^{\circ}(\text{PhO–H})$ can be derived from Eq. (10).

$$DH_{\text{sln}}^{\circ}(\text{PhO–H}) = \frac{\Delta_{\text{r}}H_2}{2} + DH_{\text{sln}}^{\circ}(t\text{-BuO–H}) \quad (10)$$

To determine the O–H bond dissociation enthalpy of *tert*-butanol in solution, several approaches can be followed. The first one uses the gas-phase value reported by DeTuri and Ervin [22], $DH^{\circ}(t\text{-BuO–H}) = 444.9 \pm 2.8\text{ kJ mol}^{-1}$, as the starting point. To estimate $DH_{\text{sln}}^{\circ}(t\text{-BuO–H})$ from that value, three solvation terms are needed, according to Eq. (11).

$$\begin{aligned} DH_{\text{sln}}^{\circ}(t\text{-BuO–H}) &= DH^{\circ}(t\text{-BuO–H}) \\ &- \Delta_{\text{sln}}H^{\circ}(t\text{-BuOH, g}) + \Delta_{\text{sln}}H^{\circ}(t\text{-BuO}^{\bullet}, \text{g}) \\ &+ \Delta_{\text{sln}}H^{\circ}(\text{H}^{\bullet}, \text{g}) \end{aligned} \quad (11)$$

The solvation of the hydrogen atom can be estimated using the hydrogen molecule as a suitable model [23], yielding $\Delta_{\text{sln}}H^{\circ}(\text{H}^{\bullet}, \text{g}) = 5 \pm 1\text{ kJ mol}^{-1}$ for organic solvents [24]. We also have recent evidence, obtained from Monte Carlo calculations, that the solvation enthalpies of H_2 and H^{\bullet} are similar within 1 kJ mol^{-1} [6]. The solvation terms for *tert*-butanol and *tert*-butoxy radical are still required, but only the former is experimentally available. Note, however, that we only need to know the difference between those quantities, $\Delta\Delta_{\text{sln}}H^{\circ}(t\text{-BuOH}/t\text{-BuO}^{\bullet}) = \Delta_{\text{sln}}H^{\circ}(t\text{-BuOH, g}) - \Delta_{\text{sln}}H^{\circ}(t\text{-BuO}^{\bullet}, \text{g})$. In recent works [1,5], this problem was solved by adopting a procedure based on Drago’s ECW model [25]. For instance, solvents like carbon tetrachloride, a weak Lewis base, will have negligible interactions both with *t*-BuOH and *t*-BuO \cdot , so that $\Delta\Delta_{\text{sln}}H^{\circ}(t\text{-BuOH}/t\text{-BuO}^{\bullet}) \approx 0$. On the other hand, a strong Lewis base solvent like acetonitrile, which is also a hydrogen bond acceptor, is able to form one hydrogen bond with *t*-BuOH. The same conclusion can be drawn for a weaker hydrogen bond acceptor like benzene. The enthalpy of this hydrogen bond will therefore be a good approximation of the difference in solvation enthalpies between the parent molecule and its radical, $\Delta\Delta_{\text{sln}}H^{\circ}(t\text{-BuOH}/t\text{-BuO}^{\bullet})$ [4]. This forms the basis of the “hydrogen bond only” model to describe solvation. By providing an estimate for the enthalpy of this hydrogen bond, the ECW model is a convenient procedure to derive $\Delta\Delta_{\text{sln}}H^{\circ}(t\text{-BuOH}/t\text{-BuO}^{\bullet})$, allowing the evaluation of $DH_{\text{sln}}^{\circ}(t\text{-BuO–H})$ from Eq. (11). The model relies on Eq. (12), which contains four parameters that reflect electrostatic ($E_{\text{A}}E_{\text{B}}$) and covalent ($C_{\text{A}}C_{\text{B}}$)

² This value is found by setting the time-constraint limit at $\tau = 60\text{ ns}$ for a 0.5 MHz transducer [30]. The rate constant for reaction 6 in benzene is $k = 3.3 \times 10^8\text{ M}^{-1}\text{ s}^{-1}$ [31].

³ The ratio between the rate constants in benzene and acetonitrile was estimated using an empirical equation given in [20] (parameters quoted from the paper by Snelgrove et al. and from Abraham et al. [32]).

⁴ If one desires to use classical PAC, the actual limit of τ below which the time-constraint is met for a given transducer is difficult to define a priori. For a 0.5 MHz transducer (response time $2\ \mu\text{s}$), Wayner et al. [4] empirically choose 100 ns as that limit, and used laser flash photolysis results to adjust the phenol concentration until the lifetime of reaction 6 was lower than that. However, as the microphone specifications are only moderately accurate, the safest way of ensuring that the time-constraint is being met is to verify it during the PAC experiment, e.g. by varying the concentration of substrate until the observed waveform reaches a maximum (or, which is equivalent, until the final value $\Delta_{\text{obs}}H$ reaches a maximum) [11]. Obviously, TR-PAC eliminates this problem.

contributions to the enthalpies of donor-acceptor interactions. Donor (B) and acceptor (A) parameters, optimized by a large database of experimentally determined enthalpies, are available for many substances [25].

$$-\Delta H(\text{ECW}) = E_A E_B + C_A C_B \quad (12)$$

Table 1 shows the calculated $\Delta\Delta_{\text{sln}}H^\circ(t\text{-BuOH}/t\text{-BuO}^\bullet) = -\Delta H(\text{ECW})$ values for each solvent studied, and the corresponding $DH_{\text{sln}}^\circ(t\text{-BuO-H})$ results.

The second approach to evaluate $DH_{\text{sln}}^\circ(t\text{-BuO-H})$ uses the solution-phase O–O bond dissociation enthalpy in di-*tert*-butylperoxide, $DH_{\text{sln}}^\circ(t\text{-BuO-OBu-}t)$, as the starting point. In a previous work [5], we have reported this enthalpy in several solvents, including benzene, through a static PAC study of reaction 5 alone. The enthalpy of this reaction, $\Delta_r H_1$, is equal to $DH_{\text{sln}}^\circ(t\text{-BuO-OBu-}t)$. The relation between both bond dissociation enthalpies is given by Eq. (13).

$$\begin{aligned} DH_{\text{sln}}^\circ(t\text{-BuO-H}) &= \Delta_f H^\circ(t\text{-BuO}^\bullet, \text{sln}) + \Delta_f H^\circ(\text{H}^\bullet, \text{sln}) \\ &- \Delta_f H^\circ(t\text{-BuOH}, \text{sln}) = \frac{DH_{\text{sln}}^\circ(t\text{-BuO-OBu-}t)}{2} \\ &+ \frac{\Delta_f H^\circ(t\text{-BuOOBu-}t, 1) + \Delta_{\text{sln}}H^\circ(t\text{-BuOOBu-}t, 1)}{2} \\ &+ \Delta_f H^\circ(\text{H}^\bullet, \text{g}) + \Delta_{\text{sln}}H^\circ(\text{H}^\bullet, \text{g}) - \Delta_f H^\circ(t\text{-BuOH}, 1) \\ &- \Delta_{\text{sln}}H^\circ(t\text{-BuOH}, 1) \end{aligned} \quad (13)$$

The required values to obtain $DH_{\text{sln}}^\circ(t\text{-BuO-H})$ are therefore the O–O bond dissociation enthalpy of di-*tert*-butylperoxide in solution, determined by PAC, together with the solution enthalpies of di-*tert*-butylperoxide and *tert*-butanol, both determined by reaction–solution calorimetry [5]. The remaining auxiliary values are the enthalpies of formation of di-*tert*-butylperoxide ($-380.9 \pm 0.9 \text{ kJ mol}^{-1}$), *tert*-butanol ($-359.2 \pm 0.8 \text{ kJ mol}^{-1}$) [26], and the hydrogen atom ($217.998 \pm 0.006 \text{ kJ mol}^{-1}$) [27]. Finally, using the same estimate for the solvation enthalpy of the hydrogen atom as above, one obtains the values for $DH_{\text{sln}}^\circ(t\text{-BuO-H})$ displayed in Table 2.

Except in the case of carbon tetrachloride, the estimates from the ECW procedure in Table 1 and the solution results

Table 1
Solution-phase bond dissociation enthalpies of *tert*-butanol, $DH_{\text{sln}}^\circ(t\text{-BuO-H})$, derived from the gas-phase value, using the ECW method (procedure 1, Eq. (11))

Solvent	$\Delta\Delta_{\text{sln}}H^\circ(t\text{-BuOH}/t\text{-BuO}^\bullet)^a$	$DH_{\text{sln}}^\circ(t\text{-BuO-H})$
C ₆ H ₆	−4.4	454.3 ± 3.1
CCl ₄	0 ^b	449.9 ± 3.1
CH ₃ CN	−9.2	459.1 ± 3.1

Data in kJ mol^{-1} . $T = 298.15 \text{ K}$.

^a Differential solvation enthalpy between the parent molecule and the radical, $\Delta\Delta_{\text{sln}}H^\circ(t\text{-BuOH}/t\text{-BuO}^\bullet) = \Delta_{\text{sln}}H^\circ(t\text{-BuOH}, \text{g}) - \Delta_{\text{sln}}H^\circ(t\text{-BuO}^\bullet, \text{g})$, identified with the enthalpy of the hydrogen bond between *tert*-butanol and the solvent, estimated by the ECW method.

^b By definition in the ECW method.

in Table 2 are in very good agreement. This was noted before, and the discrepancy in the case of carbon tetrachloride may be due to the imposition of *no* interaction between CCl₄ and the solute by the ECW model [5]. On the other hand, one would expect that $DH_{\text{sln}}^\circ(t\text{-BuO-H})$ increased when the interaction of *tert*-butanol with the solvent were larger (see Eq. (11)). While this is observed for acetonitrile, the remaining two results are similar. This observation is consistent with the weak interactions involved in the case of *tert*-butanol vs. its radical, in benzene and carbon tetrachloride. In the case of phenol, where the hydrogen bond with the solvent is stronger, that difference was expected to be larger [4].

The previous methodology illustrates how $DH_{\text{sln}}^\circ(t\text{-BuO-OBu-}t)$ can be used to derive $DH_{\text{sln}}^\circ(t\text{-BuO-H})$, which in turn affords $DH_{\text{sln}}^\circ(\text{PhO-H})$ through Eq. (10). Recall, however, that a single TR-PAC experiment can provide the enthalpy of *both* processes in Scheme 1, i.e. reactions 5 and 6. Therefore, by combining Eqs. (10) and (13), we can derive Eq. (14), where $\Delta_r H_1$ and $\Delta_r H_2$ are the enthalpies of reactions 5 and 6, respectively, determined in the *same* TR-PAC experiment.

$$\begin{aligned} DH_{\text{sln}}^\circ(\text{PhO-H}) &= \frac{(\Delta_r H_1 + \Delta_r H_2)}{2} \\ &+ \frac{\Delta_f H^\circ(t\text{-BuOOBu-}t, 1) + \Delta_{\text{sln}}H^\circ(t\text{-BuOOBu-}t, 1)}{2} \\ &+ \Delta_f H^\circ(\text{H}^\bullet, \text{g}) + \Delta_{\text{sln}}H^\circ(\text{H}^\bullet, \text{g}) \\ &- \Delta_f H^\circ(t\text{-BuOH}, 1) - \Delta_{\text{sln}}H^\circ(t\text{-BuOH}, 1) \end{aligned} \quad (14)$$

Eq. (14) corresponds to the third procedure, which has the advantage that all the solution terms can now be experimentally determined (with the exception of the solvation enthalpy of the hydrogen atom) in the *same* mixtures used in the experiment, i.e. they contain also the substrate (phenol in this case) and di-*tert*-butylperoxide. Therefore, using Eq. (14), together with the solution enthalpies of di-*tert*-butylperoxide and *tert*-butanol, measured by reaction–solution calorimetry in the actual experimental solutions, the only remaining assumption regards the hydrogen atom solvation enthalpy (see, however, below). Table 3 contains the new solution enthalpies measured in the solutions used in the TR-PAC experiments. Table 4 displays the TR-PAC measurements and collects the final results for $DH_{\text{sln}}^\circ(\text{PhO-H})$ obtained from the three procedures.

The first point to notice in Table 4 is the very good agreement in $DH_{\text{sln}}^\circ(\text{PhO-H})$ derived from the first and second procedures in each solvent, except in the case of carbon tetrachloride. This obviously stems from the corresponding values of $DH_{\text{sln}}^\circ(t\text{-BuO-H})$ used (Tables 1 and 2, respectively), and therefore such disagreement was expected. One should then leave out this case in the following comparison. On the other hand, the agreement between the results in the remaining solvents do provide useful evidence. Recall that the $DH_{\text{sln}}^\circ(\text{PhO-H})$ values in column P1 of Table 4 were derived from the gas-phase result for $DH_{\text{sln}}^\circ(t\text{-BuO-H})$ with the (small) ECW correction, while those in column

Table 2

Solution-phase bond dissociation enthalpies of *tert*-butanol, $DH_{\text{sln}}^{\circ}(t\text{-BuO-H})$, derived from procedure 2 (Eq. (13))

Solvent	$DH_{\text{sln}}^{\circ}(t\text{-BuO-OBu-}t)^a$	$\Delta_{\text{sln}}H^{\circ}(t\text{-BuOOBu-}t, 1)^a$	$\Delta_{\text{sln}}H^{\circ}(t\text{-BuOH}, 1)^a$	$DH_{\text{sln}}^{\circ}(t\text{-BuO-H})$
C ₆ H ₆	156.7 ± 9.9	1.21 ± 0.22	15.5 ± 0.4	455.2 ± 5.2
CCl ₄	164.1 ± 6.9	0.35 ± 0.04	16.2 ± 1.0	457.8 ± 3.8
CH ₃ CN	156.8 ± 6.3	5.5 ± 0.2	10.2 ± 0.5	462.7 ± 3.5

Data in kJ mol⁻¹. $T = 298.15$ K.^a Values from [5].

Table 3

Solution enthalpies of di-*tert*-butylperoxide and *tert*-butanol in the actual TR-PAC experimental solutions, determined by reaction–solution calorimetry

Solvent	[PhOH] (mM)	$\Delta_{\text{sln}}H^{\circ}(t\text{-BuOOBu-}t, 1)^a$ (kJ mol ⁻¹)	$\Delta_{\text{sln}}H^{\circ}(t\text{-BuOH}, 1)^b$ (kJ mol ⁻¹)
C ₆ H ₆	3.0	1.51 ± 0.16	15.55 ± 0.28
CCl ₄	1.4	0.17 ± 0.08	16.8 ± 0.9
CH ₃ CN	94.0	5.33 ± 0.14	9.51 ± 0.30

 $T = 298.15$ K.^a Solution enthalpies in a solution containing the indicated phenol concentration and 4–7% of di-*tert*-butylperoxide. Ampoules with the peroxide (4–8 mmol) were consecutively broken in a solution initially containing 4% of di-*tert*-butylperoxide.^b Solution enthalpies in a solution containing the indicated phenol concentration and ca. 5% of di-*tert*-butylperoxide. Ampoules with *tert*-butanol (0.3–1.7 mmol) were consecutively broken in that solution.

Table 4

TR-PAC results of solution-phase bond dissociation enthalpies of phenol, $DH_{\text{sln}}^{\circ}(\text{PhO-H})$, in various solvents, using three different procedures (see Section 3)

Solvent	[PhOH] (mM)	$\Delta_{\text{obs}}H_1^{a,b}$ (kJ mol ⁻¹)	$\Delta_{\text{obs}}H_2^{b,c}$ (kJ mol ⁻¹)	Φ_r^d	χ^e (mL kJ ⁻¹)	$DH_{\text{sln}}^{\circ}(\text{PhO-H})/\text{kJ mol}^{-1}$		
						P1 ^f	P2 ^g	P3 ^h
C ₆ H ₆	2.5	236.6 ± 5.0	124.0 ± 2.7	0.83	0.799	379.6 ± 3.5	380.5 ± 5.4 ⁱ	381.9 ± 4.5
CCl ₄	1.5	257.8 ± 5.5	110.7 ± 3.4	0.76	0.907	377.1 ± 3.8	385.0 ± 4.4	373.5 ± 5.1
CH ₃ CN	100	244.4 ± 8.9	131.8 ± 2.1	0.89	0.791	385.1 ± 3.3	388.7 ± 3.7 ⁱ	381.4 ± 5.9

 $T = 298.15$ K.^a Measured enthalpy change for the prompt process, attributed to reaction 5.^b Average of at least five experiments; the error is twice the standard deviation of the mean in each case.^c Measured enthalpy change for the sequential slower process, attributed to reaction 6.^d Data from [4].^e Data used to calculate χ from [33].^f Calculated from Eq. (10) using $DH_{\text{sln}}^{\circ}(t\text{-BuO-H})$ values from Table 1.^g Calculated from Eq. (10) using $DH_{\text{sln}}^{\circ}(t\text{-BuO-H})$ results from Table 2.^h Calculated using Eq. (14) and the solvation results in Table 3.ⁱ From [6].

P2 rely on the experimental static PAC measurement of $DH_{\text{sln}}^{\circ}(t\text{-BuO-OBu-}t)$, and thus require the knowledge of the volume change of reaction 5 (see Eq. (2)). This value was estimated from a comparison between solution and gas-phase results as $\Delta_r V_1 = 13.4 \pm 4.0$ mL mol⁻¹ (independent of solvent) [4]. The close similarity of the results obtained with procedures 1 and 2 supports this estimate for $\Delta_r V_1$.

Comparing now the results from procedures 2 and 3 for benzene and acetonitrile (Table 4), again a good agreement is observed. This is due to two reasons, the first made evident by comparing the dissolution results in Tables 2 and 3, which demonstrate that the presence of the substrate (phenol) and, more importantly, di-*tert*-butylperoxide in the experimental solution has a negligible impact on the solution enthalpies of *t*-BuOOBu-*t* and *t*-BuOH, in comparison to the values in the pure solvents. The other reason is that

the enthalpy of reaction 5 is correctly obtained by TR-PAC. As explained above, procedure 3 relies on the value of $DH_{\text{sln}}^{\circ}(t\text{-BuO-OBu-}t)$ obtained in the same experiment where $DH_{\text{sln}}^{\circ}(\text{PhO-H})$ was determined. Hence, the agreement confirms that the TR-PAC results are consistent with the ones obtained from static PAC, and that the enthalpy of the first process (reaction 5) in solution can be accurately determined by TR-PAC. However, it must be stated that this bonus is not always possible. In some experiments, the substrate may also absorb at the excitation wavelength, interfering with the measured photoacoustic signal of the photochemically active substance (di-*tert*-butylperoxide). In those cases, TR-PAC analysis will not reveal the correct enthalpy of reaction 5. However, this contribution resulting from the substrate absorption may only affect the measured amplitude of the first process, but not of the second,

Table 5
Gas-phase O–H bond dissociation enthalpy of phenol, $DH^\circ(\text{PhO-H})$, from solution data using two procedures (see Section 3)

Solvent	$DH_{\text{sln}}^\circ(\text{PhO-H})$	H bond only (ECW)		Microsolvation	
		$\Delta\Delta_{\text{sln}}H^\circ(\text{PhOH/PhO}^\bullet)$	$DH^\circ(\text{PhO-H})$	$\Delta\Delta_{\text{sln}}H^\circ(\text{PhOH/PhO}^\bullet)$	$DH^\circ(\text{PhO-H})$
C_6H_6	380.5 ± 5.4	–8.7	366.8 ± 5.6	–4.2	371.3
CCl_4	385.0 ± 4.4	0 ^a	380.0 ± 4.6		
CH_3CN	388.7 ± 3.7	–18.7	365.0 ± 4.0	–10.7	373.0

Values in kJ mol^{-1} . $T = 298.15 \text{ K}$.

^a By definition in the ECW method.

which is much slower [1]. Therefore, the amplitude of the second process, obtained from the deconvolution, will still be exclusively related to reaction 6, allowing the correct calculation of the bond dissociation enthalpy, using either procedure 1 or 2.

Before moving on to the relation between solution and gas-phase data, we must decide on which procedure is the best. Except in the case of carbon tetrachloride, all the procedures give essentially the same results. Since procedure 1 relies on an estimated bond dissociation enthalpy in solution, the other two should be preferred. Procedure 3 relies on fewer assumptions, but as procedure 2 is more general, we will adopt its results for the remainder of this work.

The relationship between the solution- and gas-phase bond dissociation enthalpies in phenol is established by Eq. (15) (analogous to Eq. (11), except that now we are deriving the gas-phase result from the solution value):

$$DH^\circ(\text{PhO-H}) = DH_{\text{sln}}^\circ(\text{PhO-H}) + \Delta_{\text{sln}}H^\circ(\text{PhOH}, \text{g}) - \Delta_{\text{sln}}H^\circ(\text{PhO}^\bullet, \text{g}) - \Delta_{\text{sln}}H^\circ(\text{H}^\bullet, \text{g}) \quad (15)$$

This equation shows that the solvation enthalpy of the hydrogen atom cancels out when the gas-phase value is calculated from the solution value (e.g. combine this equation with Eq. (13)). In other words, even if the estimate of $\Delta_{\text{sln}}H^\circ(\text{H}^\bullet, \text{g})$ is dead wrong, this will only affect the accuracy of the solution-phase bond dissociation enthalpy. The gas-phase bond dissociation enthalpy will not change, provided that the same estimate for $\Delta_{\text{sln}}H^\circ(\text{H}^\bullet, \text{g})$ is used in Eq. (15). Yet, the differential solvation between phenol and its radical, $\Delta\Delta_{\text{sln}}H^\circ(\text{PhOH/PhO}^\bullet) = \Delta_{\text{sln}}H^\circ(\text{PhOH}, \text{g}) - \Delta_{\text{sln}}H^\circ(\text{PhO}^\bullet, \text{g})$, still needs to be considered. As explained above for the case of *t*-BuOH, this quantity can be estimated using the ECW procedure, according to the “hydrogen bond only” model for solvation. Table 5 presents these estimates together with the final results for $DH^\circ(\text{PhO-H})$ (using $\Delta_{\text{sln}}H^\circ(\text{H}^\bullet, \text{g}) = 5 \pm 1 \text{ kJ mol}^{-1}$ as before).

We have recently demonstrated that the “hydrogen bond only” model may not lead to the most accurate results [6]. In the case of phenol this can be seen by comparing the values on the fourth column of Table 5 with a recommended literature value, $DH^\circ(\text{PhO-H}) = 371.3 \pm 2.3 \text{ kJ mol}^{-1}$ [24]. A more elaborate procedure to describe the solvation is the “microsolvation” or “microcluster” method, which considers that the solvated species can be modeled by gas-phase

“clusters” or “complexes”, involving a small number (usually 1–3) of solvent molecules [6,7,28]. The approach can be illustrated by using the simplest case of the solvation with a single acetonitrile molecule, taken from [7]. The computed ground state energies of phenol, acetonitrile, and a phenol–acetonitrile complex, led to $-23.1 \text{ kJ mol}^{-1}$ for the enthalpy of the interaction between PhOH and CH_3CN . But when the same exercise was carried out for the corresponding phenoxy radical we obtained $-12.4 \text{ kJ mol}^{-1}$ for the phenoxy-acetonitrile interaction. This surprisingly high value showed that the interaction of the radical with the solvent cannot be ignored, leading to a differential solvation of only $\Delta\Delta_{\text{sln}}H^\circ(\text{PhOH/PhO}^\bullet) = -10.7 \text{ kJ mol}^{-1}$, almost half of what the “hydrogen bond only” model predicted using the ECW method. While in the parent molecule the interaction is indeed dominated by the hydrogen bond with the solvent, in the radical there will be a stronger dipole–dipole interaction (phenoxy radical has a much larger dipole moment than phenol, 4.07 D versus 1.4 D, respectively) [6]. In the case of benzene, the computed differential solvation resulted in $\Delta\Delta_{\text{sln}}H^\circ(\text{PhOH/PhO}^\bullet) = -4.2 \text{ kJ mol}^{-1}$, which is closer to the ECW value, but still significantly smaller. These results and the derived $DH^\circ(\text{PhO-H})$ values in benzene and in acetonitrile are presented in Table 5. It can be seen that the agreement with the recommended gas-phase value, $DH^\circ(\text{PhO-H}) = 371.3 \pm 2.3 \text{ kJ mol}^{-1}$, improves when the differential solvation enthalpy is obtained with the microsolvation method. The “hydrogen bond only” model overestimates the magnitude of this differential interaction, and thus leads to an underestimation of $DH^\circ(\text{PhO-H})$. Note, however, that when the interactions with the solvent are weaker, this model and the ECW method can provide results in good agreement with other techniques, as demonstrated by the $DH_{\text{sln}}^\circ(t\text{-BuO-H})$ values in Tables 1 and 2. The case of carbon tetrachloride, will require further investigation, using the microsolvation and/or statistical simulation methods.

4. Summary and final comments

Like all other techniques used to probe the energetics of transient molecules, photoacoustic calorimetry also has its virtues and its problems. However, a fairly large number of PAC-derived thermochemical results have become available,

most in excellent agreement with values derived from other techniques [3]. There has been an enduring effort to improve the reliability of photoacoustic calorimetry. Nevertheless, several questions keep being raised, the most common regarding the use of di-*tert*-butylperoxide as the “universal” initiator (Scheme 1). This radical precursor is not used by all the PAC community (some preferring, for instance, benzophenone [29]), but, for several reasons, most find it advantageous over other initiators, chiefly because *t*-BuO• is a widely used and extensively studied hydrogen-acceptor (see e.g. [3]).

One of the main reasons for questioning the use of di-*tert*-butylperoxide is the amount of this compound that is required in typical PAC experiments, ca. 6% (v/v). The issue was already mentioned regarding its influence on the thermoelastic properties of the sample solution (see Section 2.2.2). As discussed, there is experimental evidence that this is not a significant problem. However, we are still in the process of finding more direct confirmation by measuring each one of the quantities present in Eq. (3), both for the experimental and calibration solutions. Preliminary results in benzene have shown that the change in χ is indeed small.⁵

It has also been argued that the amount of peroxide used could change the solvation significantly, by promoting strong interactions with both *t*-BuOH and PhOH and their radicals. However, the excellent agreement between PAC-derived bond dissociation enthalpies and gas-phase literature values [3] show that that is not the case. Furthermore, if those interactions were significant, the PAC-derived values would be sensitive to the amount of peroxide present in solution, and they are not, at least in the concentration range of 1–12% (v/v) [11,18].

Another important criticism on the use of di-*tert*-butylperoxide concerns the need for a volume change correction (Eq. (2)). As already pointed out, TR-PAC minimizes this problem in relation to classical PAC because the calculations involving $\phi_{\text{obs},2}$ refer exclusively to a reaction (reaction 6, Scheme 1) where the number of reactant molecules equals the number of product molecules, so that its volume change should be negligible. The good agreement of TR-PAC-derived bond dissociation enthalpies with reference literature values for the case of the O–H bond in phenol, S–H bond in thiophenol [1] and C–H in toluene [2], to cite but a few, strongly supports that assumption. Furthermore, the good agreement between the results presented here from procedures 2 and 3 also supports the estimated value [4] of

the volume change for the peroxide homolysis reaction (and also $\Delta_r V_2 \approx 0$ for the abstraction reaction).

The proper accounting of the solvation effects could perhaps pose the biggest threat to the accurate determination of gas-phase bond dissociation enthalpies from the solution results. Significant advances have been made in this field over the last years [4,6]. It was shown that the “hydrogen bond model” may not be the best model to describe solvation [6,7], since it neglects the interactions between the radical and the solvent, although the errors it introduces are smaller when weak interactions are involved. The microsolvation approach seems to lead to good results even with strong solvating molecules like acetonitrile. It should be noted, however, that for a correct description of solvation more elaborate procedures must be used, since the local models presented here cannot describe important features such as long-range interactions and solvent relaxation. Both these aspects are very important in the case of acetonitrile, as demonstrated by Monte Carlo simulations [6]. Yet, since we are only dealing with *differences* in solvation, the microsolvation model seems to provide good results, probably due to some error cancellation. Computational chemistry calculations will certainly play a major role in our understanding of solvation energetics.

Acknowledgements

We thank Dr. Manuel Minas da Piedade (FCUL) and Dr. Hermínio Diogo (Instituto Superior Técnico, Lisboa) for assistance with the reaction–solution calorimetry experiments. This work was supported by Fundação para a Ciência e a Tecnologia (FCT), Portugal (POCTI/35406/QUI/1999). C.F.C. and P.M.N. thank FCT for a Ph.D. (SFRH/BD/6519/2001) and a post-doctoral grant (SFRH/BPD/11465/2002), respectively.

References

- [1] R.M. Borges dos Santos, V.S.F. Muralha, C.F. Correia, R.C. Guedes, B.J. Costa Cabral, J.A. Martinho Simões, *J. Phys. Chem. A* 106 (2002) 9883.
- [2] V.S.F. Muralha, R.M. Borges dos Santos, J.A. Martinho Simões, *J. Phys. Chem. A* 108 (2004) 936.
- [3] L.J.J. Laarhoven, P. Mulder, D.D.M. Wayner, *Acc. Chem. Res.* 32 (1999) 342, and references therein.
- [4] D.D.M. Wayner, E. Luszyk, D. Pagé, K.U. Ingold, P. Mulder, L.J.J. Laarhoven, H.S. Aldrich, *J. Am. Chem. Soc.* 117 (1995) 8737.
- [5] R.M. Borges dos Santos, V.S.F. Muralha, C.F. Correia, J.A. Martinho Simões, *J. Am. Chem. Soc.* 123 (2001) 12760.
- [6] R.C. Guedes, K. Coutinho, B.J.C. Cabral, S. Canuto, C.F. Correia, R.M. Borges dos Santos, J.A. Martinho Simões, *J. Phys. Chem. A* 107 (2003) 9197.
- [7] C.F. Correia, R.C. Guedes, R.M. Borges dos Santos, B.J.C. Cabral, J.A. Martinho Simões, *Phys. Chem. Chem. Phys.* 6 (2004) 2109.
- [8] H.P. Diogo, M.E. Minas da Piedade, J.A. Martinho Simões, Y. Nagano, *J. Chem. Thermodyn.* 27 (1995) 597.
- [9] W.J. Jolly, *Inorg. Synth.* 11 (1968) 120.

⁵ We have measured C_p , ρ , and α_p for some typical PAC solutions. At 298.15 K, for a calibration solution with 1.1 mM of ferrocene and 0.163 M of phenol in benzene we obtained $\chi = 0.810 \text{ mL kJ}^{-1}$, compared with $\chi = 0.791 \text{ mL kJ}^{-1}$, determined for a typical sample solution containing approximately the same concentration of phenol (0.158 M) and 11% (v/v) of peroxide in the same solvent. Pure benzene has $\chi = 0.799 \text{ mL kJ}^{-1}$ (cf. Table 4). This 2.4% variation between sample and calibration has a negligible impact on the derived $\Delta_r H_1$ value (less than 0.4 kJ mol^{-1}).

- [10] (a) K.S. Peters, *Angew. Chem. Int. Ed. Engl.* 33 (1994) 294;
(b) S.E. Braslavsky, G.E. Heibel, *Chem. Rev.* 92 (1992) 1381;
(c) K.S. Peters, *Pure Appl. Chem.* 59 (1986) 1263.
- [11] R.M. Borges dos Santos, A.L.C. Lagoa, J.A. Martinho Simões, *J. Chem. Thermodyn.* 31 (1999) 1483.
- [12] R.R. Hung, J.J. Grabowski, *J. Am. Chem. Soc.* 114 (1992) 351.
- [13] K.B. Clark, D.D.M. Wayner, S.H. Demirdji, T.H. Koch, *J. Am. Chem. Soc.* 115 (1993) 2447.
- [14] J.E. Rudzki, J.L. Goodman, K. Peters, *J. Am. Chem. Soc.* 107 (1985) 7849.
- [15] J.R. Small, L.J. Libertini, E.W. Small, *Biophys. Chem.* 42 (1992) 29.
- [16] Sound Analysis, version 1.50D (for Windows 95), Quantum Northwest, Spokane, WA, 1999.
- [17] T. Autrey, N.S. Foster, K. Klepzig, J.E. Amonette, J.L. Daschbach, *Rev. Sci. Instrum.* 69 (1998) 2246.
- [18] K.B. Clark, D. Griller, *Organometallics* 10 (1991) 746.
- [19] H.P. Diogo, M.E. Minas da Piedade, J.A. Martinho Simões, C. Teixeira, *J. Organomet. Chem.* 632 (2001) 188, and references therein.
- [20] D.W. Snelgrove, J. Lusztyk, J.T. Banks, P. Mulder, K.U. Ingold, *J. Am. Chem. Soc.* 123 (2001) 469.
- [21] See, e.g., T. Jiao, G.-L. Leu, G.J. Farrell, T.J. Burkey, *J. Am. Chem. Soc.* 115 (2001) 4960.
- [22] (a) V.F. DeTuri, K.M. Ervin, *J. Phys. Chem. A* 103 (1999) 6911;
(b) V.F. DeTuri, K.M. Ervin, *J. Phys. Chem. A* 106 (2002) 9947.
- [23] (a) E. Roduner, D.M. Bartels, *Ber. Bunsenges. Phys. Chem.* 96 (1992) 1037;
(b) V.D. Parker, *J. Am. Chem. Soc.* 114 (1992) 7458 *ibid.* 11) (1993) 1201.
- [24] R.M. Borges dos Santos, J.A. Martinho Simões, *J. Phys. Chem. Ref. Data* 27 (1998) 707.
- [25] (a) R.S. Drago, A.P. Dadmun, G.C. Vogel, *Inorg. Chem.* 32 (1993) 2473;
(b) G.C. Vogel, R.S. Drago, *J. Chem. Ed.* 73 (1996) 701;
(c) R.S. Drago, *Applications of Electrostatic-Covalent Models in Chemistry*, Surfside, Gainesville, 1994.
- [26] J.B. Pedley, *Thermodynamic Data and Structures of Organic Compounds*, vol. 1, Thermodynamics Research Center, College Station, TX, 1994.
- [27] J.D. Cox, D.D. Wagman, V.A. Medvedev (Eds.), *CODATA Key Values for Thermodynamics*, Hemisphere, New York, 1989.
- [28] R.C. Guedes, B.J.C. Cabral, J.A. Martinho Simões, H.P. Diogo, *J. Phys. Chem. A* 104 (2000) 6062.
- [29] J. L. Goodman, in: J.A. Martinho Simões, A. Greenberg, J. F. Liebman (Eds.), *Energetics of Organic Free radicals*, SEARCH Series, vol. 4, Blackie Academic & Professional, London, 1992 (Chapter 5).
- [30] P. Mulder, O.W. Saastad, D. Griller, *J. Am. Chem. Soc.* 110 (1988) 4090.
- [31] J.A. Howard, J.C. Scaiano, H. Fischer (Eds.), *Landolt-Börnstein, New Series II/B*, Springer-Verlag, New York, 1984.
- [32] M.H. Abraham, P.L. Grellier, D. V. Prior, J.J. Morris, P.J. Taylor, *J. Chem Soc., Perkin Trans. 2* (1990) 521.
- [33] J.A. Riddick, W.B. Bunger, T.K. Sakano, *Organic Solvents. Physical Properties and Methods of Purification*, Wiley, New York, 1986.